THE JOURNAL OF PHYSICAL CHEMISTRY A

Article

pubs.acs.org/JPCA

Double C−H Bond Activation of Hydrocarbons by a Gas Phase Neutral Oxide Cluster: The Importance of Spin State

Zhe-Chen Wang, Shi Yin, and Elliot R. Bernstein*

Department of Chemistry, NSF ERC for Extreme Ultraviolet Science and Technology, Colorado State University, Fort Collins, Colorado 80523, United States

ABSTRACT: The neutral cluster V_2O_5 is generated and detected in the gas phase. Its reactivity toward butane is studied both experimentally and theoretically. Experimental results show clearly that neutral V_2O_5 can react with *n*-butane (C_4H_{10}) to generate $V_2O_5H_2$, indicating double hydrogen atom transfer from C_4H_{10} to V_2O_5 to produce C_4H_8. Further experimental evidence indicates that V_2O_5 is only partially reacted even at very high concentrations of C_4H_{10}. Density functional theory (DFT) studies show that the lowest energy triplet state of V_2O_5 is reactive toward C_4H_{10}, whereas the ground state singlet V_2O_5 is inert. Calculated results are in agreement with experimental findings, and a detailed reaction mechanism is provided. Reactions of $V_2O_5H_2$ with several oxidants are also studied theoretically to find a path to regenerate V_2O_5. Neutral $^3V_2O_5$ can also react with C_2H_6 to form $V_2O_5H_2$ and C_2H_4, but only as a minor reaction channel; the major product is the adsorption product $V_2O_5(C_2H_6)$.

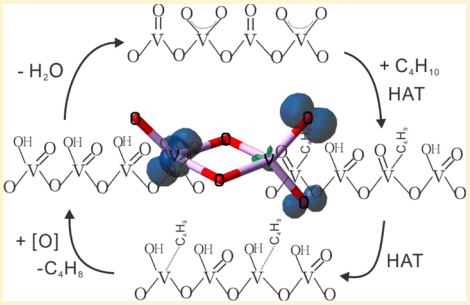

INTRODUCTION

The partially selective oxidation of light alkanes is an important process for the formation of alkenes and alkadienes, which are essential as industrial precursors for producing fuels, plastics, and many other materials.[1] Selective oxidation of *n*-butane continues to attract significant research attention, especially employing vanadium oxide (V_xO_y) related catalysts.[2] Despite intensive investigations on the surface structures of V_xO_y materials, an understanding of the distinct structures and corresponding roles of "active sites" existing on the surface of highly efficient V_xO_y catalysts is still elusive.[1]

An ideal approach for probing and understanding, at a strictly molecular level, the "active sites" on the surface of a catalyst is to study "isolated" gas phase clusters: such systems are generated in a nonperturbing environment and thus their structure and activity can be readily identified both experimentally and theoretically.[3] The crucial step for selective oxidation of light alkanes is C−H bond activation. Numerous interesting examples of C−H bond activation by ionic gas phase clusters have been reported.[3b−d,4] The C−H bond activation of methane and other small alkanes can be achieved by various gas phase cationic oxide clusters such as FeO^+,[4a,b] $(MoO_3)_{1-2}^+$,[5] OsO_4^+,[6] $(V_2O_5)_{1-5}^+$,[5b,7] MgO^+,[8] SO_2^+,[9] $P_4O_{10}^+$,[10] CuO^+,[11] GeO^+,[12] SnO^+,[12] PbO^+,[12] $(Al_2O_3)_{1,3-5}^+$,[13] $Al_2O_7^+$,[14] $(TiO_2)_{1-5}^+$,[5b,15] $(ZrO_2)_{1-4}^+$,[5b] $(HfO_2)_{1-2}^+$,[5b] $(Nb_2O_5)_{1-3}^+$,[5b] $(Ta_2O_5)_{1,2}^+$,[5b] and $Re_2O_7^+$,[5b] and anionic oxide clusters such as $ScO_{3,4}^-$,[16] $Sc_3O_6^-$,[17] $(La_2O_3)_{1-3}O^-$,[18] and $Zr_2O_8^-$.[19] In recent years, the study of binary metal oxide neutral[20] and ionic[21] clusters have also been reported. These cluster systems can serve as a more detailed molecular approach for understanding of the active sites in catalytic supports and modified catalytic systems.

Our group has developed a novel 118 nm, single photon ionization (SPI) technique, which has proved to be reliable for detecting the distribution and reactivity of *neutral* oxide clusters (NOCs) without dissociation.[22] Many gas phase NOCs and their reactivities have been studied in recent years (e.g., the reactions of vanadium, cobalt, iron, and tantalum containing NOCs with CO,[23] ethylene,[24] propylene,[24a,25] acetylene,[24b] sulfur dioxide,[26] ammonia,[27] and methanol[28]). These cluster studies yield an understanding of the corresponding condensed phase catalytic systems and enable one to propose a full catalytic cycle at the molecular level for the bulk catalytic system.

Despite the fact that the reactivity toward light hydrocarbons has been extensively studied for ionic clusters, saturated hydrocarbon activation by a NOC has yet not been reported. Herein, we report double H atom abstraction from *n*-butane by the neutral V_2O_5 cluster.

EXPERIMENTAL AND CALCULATIONAL METHODS

The experimental setup for laser ablation coupled with a fast flow reactor employed in this work has been described previously in detail:[22a,c,23−25,27−29] only a brief outline of the apparatus is given below. V_mO_n clusters are generated by laser ablation of either a mixed vanadium/cobalt target or a pure vanadium metal target in the presence of ~1% O_2 seeded in a pure helium carrier gas (99.99%, General Air). The target is either a pressed mixture of vanadium (99.5%, Sigma Aldrich) and cobalt (99.0+%, Sigma Aldrich) powders or a vanadium foil

Received: January 10, 2013
Revised: February 22, 2013
Published: February 26, 2013

   dx.doi.org/10.1021/jp400319y | *J. Phys. Chem. A* 2013, 117, 2294−2301

(99.5%, Sigma Aldrich). A 10 Hz, focused, 532 nm Nd^{3+}:YAG laser (Nd^{3+}: yttrium aluminum garnet) with 10 mJ/pulse energy is used for the laser ablation. The expansion gas is pulsed into the vacuum by a supersonic nozzle (R. M. Jordan, Co.) with a backing pressure of typically 75 psi. Generated vanadium oxide clusters react with reactants in a fast flow reactor, which is directly coupled to the cluster generation channel. The reactant gases, ethane (99.9% Sigma Aldrich), butane (99.9% Sigma Aldrich), and D-labeled butane (C_4D_{10}, 99.0% Sigma Aldrich) are used as purchased, at a 15 psi backing pressure, and injected into the reactor by a pulsed General Valve (Parker, Serial 9). The reactants and products are estimated to be thermalized to 300−400 K by collisions in the reaction cell. An electric field is placed downstream of the reactor to remove any residual ions from the molecular beam. The beam of neutral reactants and products is skimmed into a differentially pumped chamber and ionized by a separated VUV laser beam (118 nm, 10.5 eV/photon). The 118 nm laser light is generated by focusing the third harmonic (355 nm, ∼30 mJ) of a Nd^{3+}:YAG laser in a tripling cell that contains about a 250 Torr argon/xenon (10/1) gas mixture. An MgF_2 prism (Crystaltechno LTD, Russia, 6° apex angle) is placed in the laser beam to enhance separation of the generated 118 nm laser beam from the defocused 355 nm input laser beam. After the near threshold ionization, photoions are detected by a time-of-flight mass spectrometer (TOFMS).

DFT calculations are done using the Gaussian 09 program,[30] employing the hybrid B3LYP exchange−correlation functional[31] with the unrestricted Kohn−Sham solution[32] and the TZVP basis sets.[33] The unrestricted B3LYP/TZVP level of theory proved reliable in previous studies of VO_3,[21e,i,25,34] $V_2O_4^+$,[35] $V_2O_5^+$,[36] $V_3O_7^+$,[37] V_3O_8,[38] $V_4O_{10}^+$,[7a,21k] vanadium oxide anions,[39] $[OV(CH_3)_3]^+$,[40] and their gas phase reactions with small hydrocarbons. For the optimization of transition structures (TS), we employed either the Berny algorithm[41] or the synchronous transit guided quasi-Newton (STQN) method.[42] For most cases, initial approximate structures of the transition structures are obtained by relaxed potential energy surface (PES) scans using an appropriate internal coordinate. Vibrational frequencies are calculated to characterize the nature of the stationary points as minima or transition structures; the relative energies (given in electronvolts) are corrected for zero point energy (ZPE) contributions. Intrinsic reaction coordinate (IRC) calculations[43] are also performed to connect transition states (TS) with local minima. Test calculations indicate that basis set superposition error (BSSE) is negligible for these systems and thus it is not taken into account in this study.

RESULTS AND DISCUSSION

Co and V mixed metal powders (molar ratio 1:1) are pressed to form a solid metal disk to provide Co or V related signals. Figure 1a shows the distribution of neutral V_xO_y, Co_xO_y, and $V_xCo_yO_z$ clusters within the range of $155 < m/z < 200$.[20] The reactions of V_2O_5 NOC with C_4H_{10} and C_4D_{10} are studied (Figure 1b,c). For all clusters generated employing a Co/V mixed target, V_2O_5 is the only species observed to react with C_4H_{10} to generate the double hydrogen abstraction products $V_2O_5H_2$ (Figure 1b) and C_4H_8:

$$V_2O_5 + C_4H_{10} \rightarrow V_2O_5H_2 + C_4H_8 \quad (1)$$

This reaction has been further substantiated for C_4D_{10} gas, for which the deuterated product peak $V_2O_5D_2$ can be observed

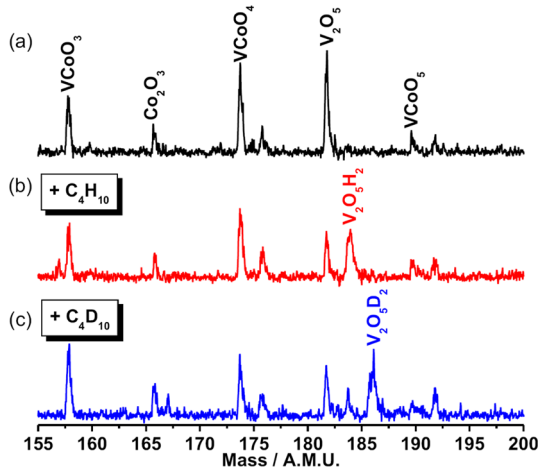

Figure 1. Gas phase V_2O_5 neutral cluster reacts with butane and deuterated butane: (a) distribution without any reactant; (b) C_4H_{10} added into the reaction cell; (c) C_4D_{10} added into the reaction cell. A V−Co target is employed to generate the signals.

(Figure 1c). The mass spectrum is very sensitive to experimental conditions, and the three spectra in Figure 1 are recorded at well controlled "identical" conditions except for the introduction of reactant gas for the lower two spectra. The experimental results shown in Figure 1 are highly repeatable using either a mixed or pure vanadium target.

Increasing the concentration of reactant gas C_4H_{10} does not, however, increase the $V_2O_5/V_2O_5H_2$ peak intensity ratio (Figure 2). One possible reason for this phenomenon is that

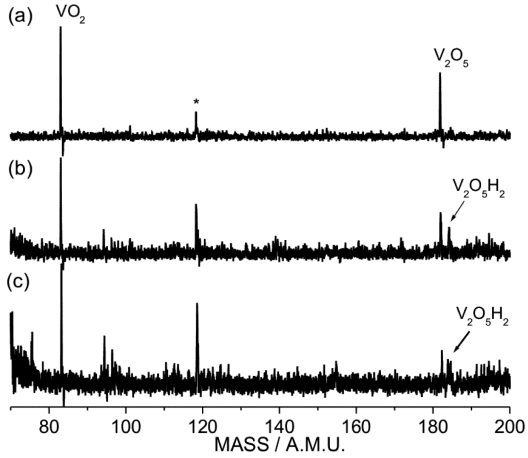

Figure 2. Generation (a) and reaction of gas phase V_2O_5 neutral cluster with butane in the pressure of (b) 3.6 Pa and (c) 7.2 Pa. A pure vanadium target is employed for the experiments. The asterisk indicates an impurity associated with the vacuum system.

we may generate a mixture of ground state and excited state V_2O_5 clusters at the same time in the cluster beam and only the excited (hot) V_2O_5 can react with C_4H_{10}. Because V_2O_5 is only partially reacted, the pseudo-first-order reaction rate constant cannot be determined for reaction 1.

The reaction of V_2O_5 with saturated hydrocarbon C_2H_6 has been reported by our group and the adsorption of C_2H_6 on V_2O_5: the product $V_2O_5(C_2H_6)$ has been identified, as given in reaction 2.[24b]

dx.doi.org/10.1021/jp400319y | J. Phys. Chem. A 2013, 117, 2294−2301

$$V_2O_5 + C_2H_6 \rightarrow V_2O_5(C_2H_6) \qquad \Delta H_{0K} = -0.65 \text{ eV} \tag{2}$$

The signal intensity of $V_2O_5(C_2H_6)$ is less than one-tenth that of the V_2O_5 parent peak. The low population of the $V_2O_5(C_2H_6)$ product can be due to the low pressure of C_2H_6 reactant gas in reaction cell during the experiments.[24b] In current work, we increased the concentration of C_2H_6 reactant gas in the flow cell. The $V_2O_5(C_2H_6)$ can still be detected as a major product while we also observe the generation of $V_2O_5H_2$ as a minor product, as given by

$$V_2O_5 + C_2H_6 \rightarrow V_2O_5H_2 + C_2H_4 \tag{3}$$

More interesting information concerning this chemistry is revealed through density functional theory (DFT) calculations to model this gas phase neutral cluster reaction system. The electronic structure of neutral V_2O_5 has been reported and the V_2O_5 lowest triplet state is 0.71 eV higher in energy than its singlet ground state at the B3LYP/TZVP level of theory.[24b] The energy difference between the V_2O_5 lowest triplet state and its singlet ground state at the CCSD(T)/TZVP level of theory (single point calculation based on fully optimized structures at the B3LYP/TZVP level of theory) is 1.36 eV, higher than the reported value (0.71 eV) at the DFT level. The larger singlet−triplet splitting could favor the trapping of the two different states as the species cool in the expansion and reaction flow tube. We calculate the potential energy surface (PES) for the reaction of C_4H_{10} with both the singlet ground state $^1V_2O_5$ and the lowest triplet state $^3V_2O_5$, respectively (Figures 3 and 4).

Figure 3 shows that C_4H_{10} can readily form a cluster with singlet ground state $^1V_2O_5$. The first step for the reaction of

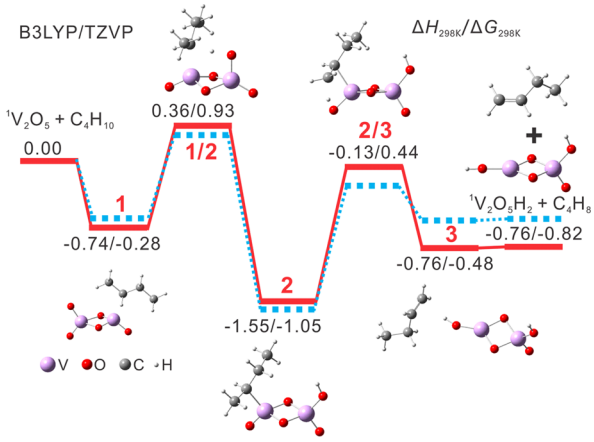

Figure 3. Calculated singlet energetic of the reaction of ground state $^1V_2O_5$ with C_4H_{10} (red solid lines) based on energy differences between the stationary and transition states at the B3LYP/TZVP level of theory. The energy values are relative to the entrance channel, denoted as reaction thermal enthalpy (ΔH_{298K}) and Gibbs free energy (ΔG_{298K}), and given in electronvolts. The ΔH_{298K} values are used to plot the PES. The blue dotted lines denote the similar PES for the reaction of ground state $^1V_2O_5$ with C_2H_6.

C_4H_{10} with $^1V_2O_5$ is to form a $^1V_2O_5(C_4H_{10})$ complex with an energy release of 0.74 eV. A further H atom transfer (HAT) process from a β-H of C_4H_{10} to one terminal oxygen atom (denoted as O_t) of the $O_bO_bVO_tO_t$ moiety of $^1V_2O_5$ (O_b: bridging oxygen) takes place with a considerable barrier of 0.36 eV. After the first HAT, the following second HAT and the C_4H_8 moiety evaporation processes are barrierless. The barrier for the first HAT indicates that the double HATs for reaction 1 cannot occur on the singlet potential energy surface. We also consider other processes for the first HAT: (1) activation of α-H of C_4H_{10} instead of β-H; (2) HAT to the O_b atom or O_t atom of $O_bO_bVO_t$ moiety; (3) first breaking the VOVO four-membered ring and then performing HAT. All these other processes show higher barriers and thus cannot help to reduce the barrier for the whole singlet reaction PES. The calculated results for the reaction of C_2H_6 with $^1V_2O_5$ show similar properties (see the blue dotted lines in Figure 3).

Figure 4 is a plot of the PES for the reaction of C_4H_{10} with the lowest energy triplet state, $^3V_2O_5$. The first HAT process

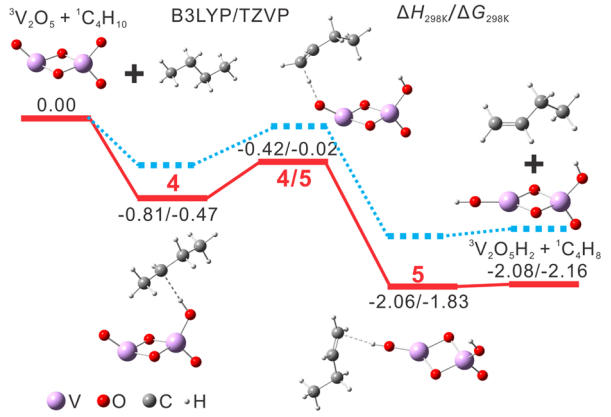

Figure 4. Calculated triplet energetic of the reaction of lowest energy triplet $^3V_2O_5$ with C_4H_{10} (red solid lines) based on energy differences between the stationary and transition states at the B3LYP/TZVP level of theory is plotted. The energy values are relative to the entrance channel, denoted as reaction thermal enthalpy (ΔH_{298K}) and Gibbs free energy (ΔG_{298K}), and given in electronvolts. The ΔH_{298K} values are used to plot the PES. The blue dotted lines denote the similar PES for the reaction of lowest energy triplet $^3V_2O_5$ with C_2H_6.

from one β-H of C_4H_{10} to the spin located O_t of $^3V_2O_5$ is overall barrierless. The formation of $^3V_2O_5H{\cdot}C_4H_9$ (**4**) is facile and straightforward. Similar HAT reactions have been reported as a spin driven process in ionic reaction systems.[3b,7a,21f] The following step goes smoothly without barrier to generate the double HAT products C_4H_8 and $^3V_2O_5H_2$. Both 1-butene and 2-butene are easily formed on the basis of a similar reaction mechanism, but due to the very weak product signals, it is almost impossible to determine the product ratio experimentally via employing D-labeled reactant such as $CD_3CH_2CH_2CD_3$. The reaction of C_2H_6 with $^3V_2O_5$ is similar to that of C_4H_{10} (see blue dotted lines in Figure 4).

The detailed DFT studies of the reaction of C_4H_{10} with ground state $^1V_2O_5$ and lowest energy $^3V_2O_5$ provide an explanation of the experimental phenomena shown in Figures 1 and 2: the coexistence of $^1V_2O_5$ (ground state V_2O_5) and $^3V_2O_5$ (excited V_2O_5) in the reaction cell might be expected during the experiments. We employ a focused 532 nm laser onto the metal disk target to generate vanadium oxide species. The temperature of generated plasma is initially high and eventually cooled by collisions with expanding room temperature carrier gas and gas in the reaction flow tube. This process is very complex and can enable trapping of different spin states and thereby favors the coexistence of $^1V_2O_5$ (ground state V_2O_5) and $^3V_2O_5$ (excited V_2O_5) in the flow tube reaction cell. This can explain why (Figure 2) neutral V_2O_5 can only partially react with C_4H_{10}.

dx.doi.org/10.1021/jp400319y | J. Phys. Chem. A 2013, 117, 2294−2301

Further theoretical investigations explore the electronic details of the mechanism concerning the difference in reactivity of $^1V_2O_5$ and $^3V_2O_5$ toward C_4H_{10}. Figure 5a shows the

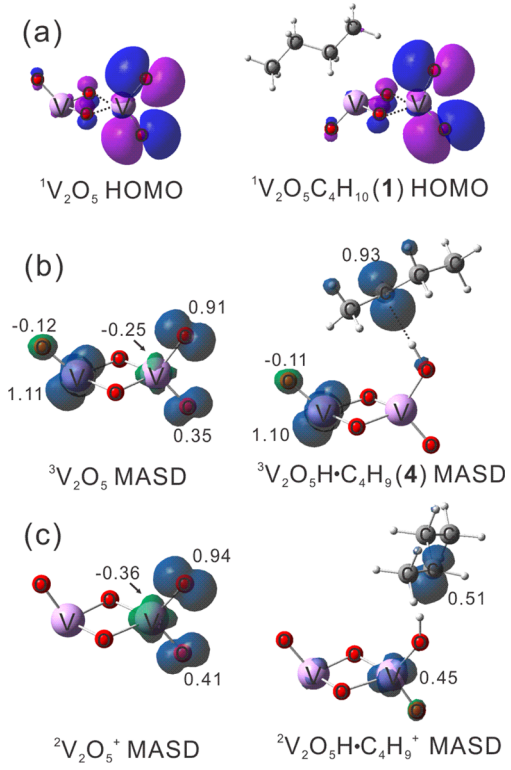

Figure 5. (a) Highest occupied molecular orbitals (HOMO) for single neutral V_2O_5 and the corresponding $^1V_2O_5C_4H_{10}$ (**1**) encounter complex and Mulliken atomic spin density (MASD) distributions for both (b) neutral $^3V_2O_5$ and $^3V_2O_5H{\cdot}C_4H_9$ (**4**) and (c) cationic doublet $^2V_2O_5^+$ and $^2V_2O_5H{\cdot}C_4H_9^+$. Note that the structure of $^2V_2O_5H{\cdot}C_4H_9^+$ cannot be located as a local minimum and the MASD plot of $^2V_2O_5H{\cdot}C_4H_9^+$ is based on a single point calculation.

changing of the highest occupied molecular orbital (HOMO) for closed-shell $^1V_2O_5$ and the formed $^1V_2O_5C_4H_{10}$ (**1**) complex. The shape of the HOMO located on the $O_bO_bVO_tO_t$ moiety does not change after the formation of $^1V_2O_5C_4H_{10}$ (**1**). To form the $^3V_2O_5H{\cdot}C_4H_9$ (**4**) isomer, however, the localized spin distribution changes from the $O_bO_bVO_tO_t$ (O_t) moiety of $^3V_2O_5$ to a β-C atom of the $^3V_2O_5H{\cdot}C_4H_9$ (**4**) isomer (Figure 5b): this spin density transfer strongly suggests a spin-driven process. One can compare neutral $^3V_2O_5$ with cationic $^2V_2O_5^+$: the latter has been reported to be very reactive toward C−H bond activation.[5b] The spin distributions of neutral $^3V_2O_5$ and cationic $^2V_2O_5^+$ are very similar in terms of the $O_bO_bVO_tO_t$ moiety, despite another unpaired electron located on the other V atom of neutral $^3V_2O_5$ (Figure 5b,c). Although the local charge effects[21f] might influence the reactivity of $^3V_2O_5$ with respect to $^2V_2O_5^+$, the spin located $O_t^\bullet$ atom plays the major role in the C−H activation behavior of neutral $^3V_2O_5$, similar to that found for ionic systems.[3b,5b,36a,44] No unpaired spin distribution exists for the singlet, closed shell, neutral $^1V_2O_5$ cluster, even though the singlet ground state $^1V_2O_5$ has a similar structure to that of the lowest energy triplet $^3V_2O_5$ isomer. Due to the spin located terminal oxygen radical, $^3V_2O_5$ is more reactive than $^1V_2O_5$ toward butane. Activation of small hydrocarbons by gas phase ionic clusters has also been noted and discussed in terms of the very important role of spin located, terminal oxygen radicals.[3b,45] On the basis of experimental and theoretical studies for methane C−H bond activation, all active metal oxide radical cations exhibit high spin densities at a terminal oxygen atom.[3b] In a parallel fashion, on the basis of the present experimental and theoretical results, we propose that neutral metal oxide clusters with terminal oxygen centered, localized spin density can also be effective toward homolytic C−H bond activation.

We calculate, at the B3LYP/TZVP level, the thermodynamics for the reaction of $^3V_2O_5H_2$ and oxidants to regenerate $^3V_2O_5$, using reactions 4 and 5:

$$^3V_2O_5H_2 + O_3 \rightarrow {}^1V_2O_5 + H_2O + O_2$$
$$\Delta H_{298K} = -1.69 \text{ eV}, \Delta G_{298K} = -2.01 \text{ eV} \quad (4)$$

$$^3V_2O_5H_2 + H_2O_2 \rightarrow {}^3V_2O_5 + 2H_2O$$
$$\Delta H_{298K} = -0.05 \text{ eV}, \Delta G_{298K} = -0.41 \text{ eV} \quad (5)$$

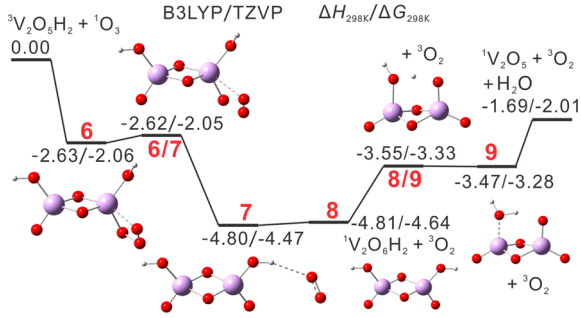

Figure 6. Calculated triplet energetic of reaction of the lowest energy triplet $^3V_2O_5H_2$ with O_3 based on energy differences between the stationary and transition states at the B3LYP/TZVP level of theory is plotted. The energy values are relative to the entrance channel, denoted as reaction thermal enthalpy (ΔH_{298K}) and Gibbs free energy (ΔG_{298K}), and given in electronvolts. The ΔH_{298K} values are used to plot the PES.

The detailed reaction mechanism for reaction 4 is shown in Figure 6. The approaching of O_3 to the less bonded V site of $^3V_2O_5H_2$ is straightforward and provides large energy release (−2.63 eV) to form a very stable encounter complex $^3V_2O_5H_2{\cdot}O_3$ (structure **6**). Then the cleavage of one O−O bond of the O_3 moiety occurs easily and leads to formation of an O_2 moiety (**6** → **6/7** → **7**). The primary products $^1V_2O_6H_2$ (**8**) and $^3O_2$ can be formed after the elimination of O_2 from **7**. Isomerization of $^1V_2O_6H_2$ (**8**) is subject to a HAT process to form the H_2O moiety in $^1V_2O_6H_2$ (**9**). The final products are formed by evaporation of the H_2O moiety. This whole process is overall barrierless while changing the multiplicity of the V containing species (from triplet $^3V_2O_5H_2$ to singlet $^1V_2O_5$). The regeneration of $^3V_2O_5$ might be achieved by photoexcitation.

Another example concerns the detailed mechanism for reaction 5, by which the regeneration of triplet $^3V_2O_5$ has been achieved (see Figure 7 for details). As shown in Figure 7, the encounter complex $^3V_2O_5H_2{\cdot}H_2O_2$ (**10**) is formed with −0.81 eV energy release and the following steps for generating the primary reaction products $^3V_2O_6H_2$ (**14**) and H_2O are

dx.doi.org/10.1021/jp400319y | J. Phys. Chem. A 2013, 117, 2294−2301

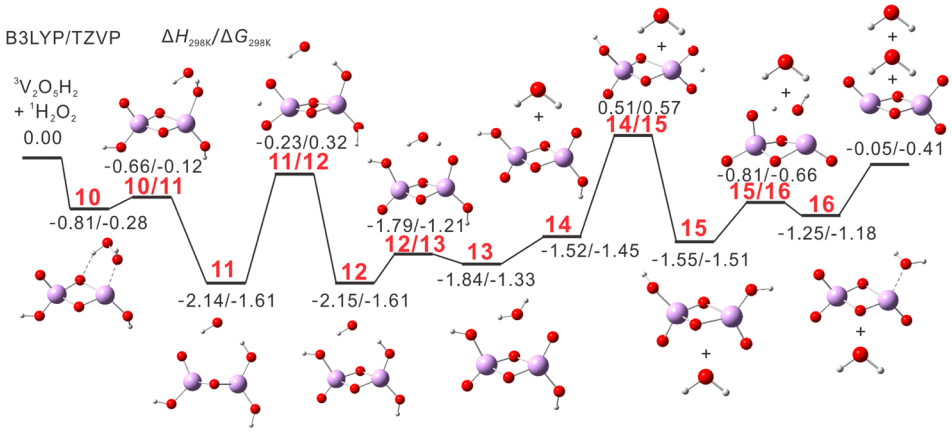

Figure 7. Calculated triplet energetic of the reaction of lowest energy triplet $^3V_2O_5H_2$ with H_2O_2 based on energy differences between the stationary and transition states at the B3LYP/TZVP level of theory is plotted. The energy values are relative to the entrance channel, denoted as reaction thermal enthalpy (ΔH_{298K}) and Gibbs free energy (ΔG_{298K}), and given in electronvolts. The ΔH_{298K} values are used to plot the PES.

barrierless (**10** → **10/11** → **11** → **11/12** → **12**→ **12/13** → **13** → **13/14** → **14**). However, to produce the second H_2O product, the essential isomerization steps of $^3V_2O_6H_2$ requiring two HAT processes (**14** → **14/15** → **15** → **15/16** → **16**) show a barrier of 0.51 eV. This detailed mechanism indicates that using a hydrogen containing oxidant might increase the chance of introducing high barriers for the catalytic cycle.

The full catalytic cycle can be achieved by combining reaction 1 with 4 and 5, which leads to reactions 6 and 7, respectively:

$$C_4H_{10} + O_3 \rightarrow C_4H_8 + H_2O + O_2$$
$$\Delta H_{298K} = -3.05 \text{ eV}, \Delta G_{298K} = -3.49 \text{ eV} \quad (6)$$

$$C_4H_{10} + H_2O_2 \rightarrow C_4H_8 + 2H_2O$$
$$\Delta H_{298K} = -2.13 \text{ eV}, \Delta G_{298K} = -2.57 \text{ eV} \quad (7)$$

Other oxidants, such as O_2 and N_2O, might also be applied to enable the complete catalytic cycle; however, according to our calculations, the regeneration of $^3V_2O_5$ by reaction of O_2 or N_2O with $^3V_2O_5H_2$ either is diminished by high barriers or is endothermic in the gas phase. Another situation arises for the reaction of O_2 with $^3V_2O_5H_2$: the regeneration of $^3V_2O_5$ cannot be directly achieved, because the primary products are V_2O_6 and H_2O. One possible resolution of this problem is for O_2 to react simultaneously (i.e., within a collision complex time) with two $^3V_2O_5H_2$ clusters: regeneration of two V_2O_5 clusters and two H_2O molecules can be realized under these conditions. The reaction of O_2 with two $^3V_2O_5H_2$ in the gas phase might be possible and would be especially interesting when the similar situation occurs on the surface of the condensed phase, where the active sites could be two neighboring $V_2O_5H_2$ moieties. The reaction of N_2O with $^3V_2O_5H_2$ to regenerate $^3V_2O_5$ with N_2 and H_2O is only slightly exothermic but shows significant barriers according to our calculations. In this case, increasing the internal energy of the reaction system or utilizing the energy from the first catalytic cycle is a potential protocol to overcome the barriers. These two model reaction systems are particularly interesting regarding both the gas phase and "active sites" on the surface of a solid catalyst.

The standard heat of formation (ΔH_f^o) of water is also calculated employing the B3LYP/TZVP level of theory: a value of −213 kJ/mol (2.23 eV) is obtained, which agrees with the experimental result of −242 kJ/mol (2.53 eV). More accurate results can be obtained with a higher level of theory, such as MP2/6-311++g**, which gives a ΔH_f^o value of −237 kJ/mol (2.48 eV): even more accurate values can be obtained by still higher levels of theory, such as CCSD(T). The B3LYP/TZVP theory level should be sufficient to indicate that the regeneration of V_2O_5 is likely by some oxidants, as shown in reactions 4 and 5 at room temperature. More accuracy can certainly be obtained by using highly accurate methods such as CCSD(T). In catalytic processes, the high spin states can be transiently induced by irradiation. An ideal mechanism on the surface of a solid V_xO_y catalyst can be provided, on the basis of the catalytic cycle shown in reactions 6 and 7, which may shed light on understanding the corresponding real catalysis on the surface of solid V_xO_y materials at the molecular level (see Figure 8 for details).

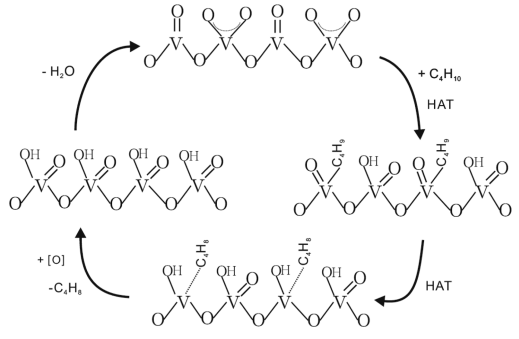

Figure 8. Proposed schematic mechanism for the oxidation of C_4H_{10} by oxidants catalyzed by vanadium oxide materials.

The ideal catalytic cycle for the C_4H_{10} oxidation on a V_xO_y catalyst is based on the reaction of C_4H_{10} with lowest energy $^3V_2O_5$ neutral cluster: (1) C_4H_{10} is chemically adsorbed on the surface of V_xO_y via the first HAT to the VO_tO_t moiety; (2) the first HAT provides enough energy for the second HAT from the C_4H_9 moiety to O_t atom of the oxygen poor VO_t moiety and the formed C_4H_8 is weakly absorbed on the V site of the VO_t moiety; (3) the C_4H_8 is released when the absorption of oxidants occurs; (4) formation and loss of a H_2O moiety is necessary to complete the proposed catalytic cycle (Figure 8).

dx.doi.org/10.1021/jp400319y | J. Phys. Chem. A 2013, 117, 2294−2301

CONCLUSIONS

The neutral oxide cluster V_2O_5 is generated and its reactivity with C_4H_{10} is studied. Experimental data suggest that V_2O_5 can react with C_4H_{10} to produce $V_2O_5H_2$ and C_4H_8. Further experimental results indicate that only a part of the V_2O_5 distribution displays this reactivity. DFT calculations suggest that the V_2O_5 cluster distribution can contain both the singlet ground electronic state and the triplet excited state cluster. A hydrogen atom transfer from C_4H_{10} to the spin located O_t site of excited state $^3V_2O_5$ is overall barrierless, whereas a hydrogen atom transfer from C_4H_{10} to singlet ground state $^1V_2O_5$ shows a significant barrier. The HAT reaction of C_2H_6 with V_2O_5 displays similar behavior to that of C_4H_{10} and DFT results parallel the experimental data, as well. The reactions of $V_2O_5H_2$ with several oxidants are exothermic and the reaction mechanisms are studied in detail to regenerate $^3V_2O_5$. A catalytic cycle for the reaction is presented and a catalytic mechanism on the surface of a condensed phase V_xO_y catalyst is proposed. Our studies not only provide new insights into gas phase reactions but also shed light on catalytic processes on the surfaces of condensed phase supported catalysts.

AUTHOR INFORMATION

Corresponding Author

*Phone: 970-491-6347. E-mail: erb@lamar.colostate.edu.

Author Contributions

The manuscript was written through contributions of all authors. All authors have given approval to the final version of the manuscript.

Notes

The authors declare no competing financial interest.

ACKNOWLEDGMENTS

This work is supported in part by grants from the U.S. Air Force Office of Scientific Research (AFOSR) through grant number FA9550-10-1-0454, the NSFERC for Extreme Ultraviolet Science and Technology under NSF Award No. 0310717, and XSEDE supercomputer resources provided by SDSC under grant number TG-CHE110083.

REFERENCES

(1) McGregor, J.; Huang, Z.; Shiko, G.; Gladden, L. F.; Stein, R. S.; Duer, M. J.; Wu, Z.; Stair, P. C.; Rugmini, S.; Jackson, S. D. The Role of Surface Vanadia Species in Butane Dehydrogenation over VO_x/Al_2O_3. *Catal. Today* **2009**, *142*, 143−151.

(2) (a) Fernandez, J. R.; Vega, A.; Diez, F. V. Partial Oxidation of n-Butane to Maleic Anhydride over VPO in a Simulated Circulating Fluidized Bed Reactor. *Appl. Catal. A-Gen.* **2010**, *376*, 76−82. (b) Taufiq-Yap, Y. H.; Goh, C. K.; Hutchings, G. J.; Dummer, N.; Bartley, J. Dependence of n-Butane Activation on Active Site of Vanadium Phosphate Catalysts. *Catal. Lett.* **2009**, *130*, 327−334. (c) Feng, R. M.; Yang, X. J.; Ji, W. J.; Chen, Y.; Au, C. T. VPO Catalysts Supported on H_3PO_4-Treated ZrO_2 Highly Active for n-Butane Oxidation. *J. Catal.* **2007**, *246*, 166−176. (d) Pierini, B. T.; Lombardo, E. A. Cr, Mo and W Used as VPO Promoters in the Partial Oxidation of n-Butane to Maleic Anhydride. *Catal. Today* **2005**, *107−08*, 323−329. (e) Wang, X. S.; Nie, W. Y.; Ji, W. J.; Guo, X. F.; Yan, Q. J.; Chen, Y. A Good Performance VPO Catalyst for Partial Oxidation of n-Butane to Maleic Anhydride. *Chem. Lett.* **2001**, 696−697.

(3) (a) Dietl, N.; Schlangen, M.; Schwarz, H. Thermal Hydrogen-Atom Transfer from Methane: The Role of Radicals and Spin States in Oxo-Cluster Chemistry. *Angew. Chem., Int. Ed.* **2012**, *51*, 5544−5555. (b) Schwarz, H. Chemistry with Methane: Concepts Rather than Recipes. *Angew. Chem., Int. Ed.* **2011**, *50*, 10096−10115. (c) Böhme, D. K.; Schwarz, H. Gas-Phase Catalysis by Atomic and Cluster Metal Ions: The Ultimate Single-Site Catalysts. *Angew. Chem., Int. Ed.* **2005**, *44*, 2336−2354. (d) Yin, S.; Bernstein, E. R. Gas Phase Chemistry of Neutral Metal Clusters: Distribution, Reactivity and Catalysis. *Int. J. Mass Spectrom.* **2012**, *321−322*, 49−65.

(4) (a) Schröder, D.; Schwarz, H. $FeO^{\oplus}$ Activates Methane. *Angew. Chem., Int. Ed.* **1990**, *29*, 1433−1434. (b) Schwarz, H. Activation of Methane. *Angew. Chem., Int. Ed.* **1991**, *30*, 820−821. (c) Schroder, D.; Schwarz, H.; Clemmer, D. E.; Chen, Y. M.; Armentrout, P. B.; Baranov, V. I.; Bohme, D. K. Activation of Hydrogen and Methane by Thermalized FeO^+ in the Gas Phase as Studied by Multiple Mass Spectrometric Techniques. *Int. J. Mass Spectrom. Ion Processes* **1997**, *161*, 175−191. (d) Zhao, X.; Hopkinson, A. C.; Bohme, D. K. Competitive Activation of C-H and C-X Bonds in Reactions of Pt^+ with CH_3X (X = F,Cl): Experiment and Theory. *ChemPhysChem* **2008**, *9*, 873−881. (e) Bozovic, A.; Böhme, D. K. Activation of X-H and X-D Bonds (X = O, N, C) by Alkaline-Earth Metal Monoxide Cations: Experiment and Theory. *Phys. Chem. Chem. Phys.* **2009**, *11*, 5940−5951. (f) Shayesteh, A.; Lavrov, V. V.; Koyanagi, G. K.; Bohme, D. K. Reactions of Atomic Cations with Methane: Gas Phase Room-Temperature Kinetics and Periodicities in Reactivity. *J. Phys. Chem. A* **2009**, *113*, 5602−5611. (g) Bozovic, A.; Feil, S.; Koyanagi, G. K.; Viggiano, A. A.; Zhang, X. H.; Schlangen, M.; Schwarz, H.; Bohme, D. K. Conversion of Methane to Methanol: Nickel, Palladium, and Platinum (d(9)) Cations as Catalysts for the Oxidation of Methane by Ozone at Room Temperature. *Chem.—Eur. J.* **2010**, *16*, 11605−11610.

(5) (a) Kretzschmar, I.; Fiedler, A.; Harvey, J. N.; Schröder, D.; Schwarz, H. Effects of Sequential Ligation of Molybdenum Cation by Chalcogenides on Electronic Structure and Gas-Phase Reactivity. *J. Phys. Chem. A* **1997**, *101*, 6252−6264. (b) Zhao, Y. X.; Wu, X. N.; Wang, Z. C.; He, S. G.; Ding, X. L. Hydrogen-Atom Abstraction from Methane by Stoichiometric Early Transition Metal Oxide Cluster Cations. *Chem. Commun.* **2010**, *46*, 1736−1738.

(6) Irikura, K. K.; Beauchamp, J. L. Osmium Tetroxide and its Fragment Ions in the Gas Phase: Reactivity with Hydrocarbons and Small Molecules. *J. Am. Chem. Soc.* **1989**, *111*, 75−85.

(7) (a) Feyel, S.; Döbler, J.; Schröder, D.; Sauer, J.; Schwarz, H. Thermal Activation of Methane by Tetranuclear $[V_4O_{10}]^+$. *Angew. Chem., Int. Ed.* **2006**, *45*, 4681−4685. (b) Wende, T.; Dobler, J.; Jiang, L.; Claes, P.; Janssens, E.; Lievens, P.; Meijer, G.; Asmis, K. R.; Sauer, J. Infrared Spectroscopic Characterization of the Oxidative Dehydrogenation of Propane by $V_4O_{10}^+$. *Int. J. Mass Spectrom.* **2010**, *297*, 102−106. (c) Justes, D. R.; Castleman, A. W.; Mitric, R.; Bonacic-Koutecky, V. $V_2O_5^+$ Reaction with C_2H_4: Theoretical Considerations of Experimental Findings. *Eur. Phys. J. D* **2003**, *24*, 331−334.

(8) (a) Schröder, D.; Roithová, J. Low-Temperature Activation of Methane: It also Works without a Transition Metal. *Angew. Chem., Int. Ed.* **2006**, *45*, 5705−5708. (b) Schroder, D.; Roithova, J.; Alikhani, E.; Kwapien, K.; Sauer, J. Preferential Activation of Primary C-H Bonds in the Reactions of Small Alkanes with the Diatomic MgO^+ Cation. *Chem.—Eur. J.* **2010**, *16*, 4110−4119. (c) Kwapien, K.; Sierka, M.; Dobler, J.; Sauer, J. Reactions of H_2, CH_4, C_2H_6, and C_3H_8 with $(MgO)_n^+$ Clusters Studied by Density Functional Theory. *ChemCatChem* **2010**, *2*, 819−826.

(9) (a) de Petris, G.; Cartoni, A.; Troiani, A.; Barone, V.; Cimino, P.; Angelini, G.; Ursini, O.; Double, C-H Activation of Ethane by Metal-Free SO_2^+ Radical Cations. *Chem.—Eur. J.* **2010**, *16*, 6234−6242. (b) de Petris, G.; Troiani, A.; Rosi, M.; Angelini, G.; Ursini, O. Methane Activation by Metal-Free Radical Cations: Experimental Insight into the Reaction Intermediate. *Chem.—Eur. J.* **2009**, *15*, 4248−4252.

(10) (a) Dietl, N.; Engeser, M.; Schwarz, H. Competitive Hydrogen-Atom Abstraction versus Oxygen-Atom and Electron Transfers in Gas-Phase Reactions of $[X_4O_{10}]^+$ (X = P, V) with C_2H_4. *Chem.—Eur. J.* **2010**, *16*, 4452−4456. (b) Dietl, N.; Engeser, M.; Schwarz, H.; Room-Temperature, C-H Bond Activation of Methane by Bare $[P_4O_{10}]^+$. *Angew. Chem., Int. Ed.* **2009**, *48*, 4861−4863. (c) Dietl, N.; Engeser, M.; Schwarz, H. Thermal Homo- And Heterolytic C-H Bond

Activation of Ethane and Propane by Bare $[P_4O_{10}]^{\cdot+}$: Regioselectivities, Kinetic Isotope Effects, and Density Functional Theory Based Potential-Energy Surfaces. *Chem.—Eur. J.* **2009**, *15*, 11100−11104.
(11) Dietl, N.; van der Linde, C.; Schlangen, M.; Beyer, M. K.; Schwarz, H. Diatomic [CuO]+ and Its Role in the Spin-Selective Hydrogen- and Oxygen-Atom Transfers in the Thermal Activation of Methane. *Angew. Chem., Int. Ed.* **2011**, *50*, 4966−4969.
(12) Chen, K.; Wang, Z.-C.; Schlangen, M.; Wu, Y.-D.; Zhang, X.; Schwarz, H. Thermal Activation of Methane and Ethene by Bare MO^+ (M=Ge, Sn, and Pb): A Combined Theoretical/Experimental Study. *Chem.—Eur. J.* **2011**, *17*, 9619−9625.
(13) (a) Wang, Z.-C.; Dietl, N.; Kretschmer, R.; Ma, J.-B.; Weiske, T.; Schlangen, M.; Schwarz, H. Direct Conversion of Methane into Formaldehyde Mediated by $[Al_2O_3]^{\cdot+}$ at Room Temperature. *Angew. Chem., Int. Ed.* **2012**, *51*, 3703−3707. (b) Feyel, S.; Döbler, J.; Höckendorf, R.; Beyer, Martin K.; Sauer, J.; Schwarz, H. Activation of Methane by Oligomeric $(Al_2O_3)_x^+$ (x = 3, 4, 5): The Role of Oxygen-Centered Radicals in Thermal Hydrogen-Atom Abstraction. *Angew. Chem., Int. Ed.* **2008**, *47*, 1946−1950.
(14) Wang, Z.-C.; Weiske, T.; Kretschmer, R.; Schlangen, M.; Kaupp, M.; Schwarz, H. Structure of the Oxygen-Rich Cluster Cation $Al_2O_7^+$ and its Reactivity toward Methane and Water. *J. Am. Chem. Soc.* **2011**, *133*, 16930−16937.
(15) Harvey, J. N.; Diefenbach, M.; Schröder, D.; Schwarz, H. Oxidation Properties of the Early Transition-Metal Dioxide Cations MO_2^+ (M = Ti, V, Zr, Nb) in the Gas-Phase. *Int. J. Mass Spectrom.* **1999**, *182*, 85−97.
(16) Tian, L. H.; Zhao, Y. X.; Wu, X. N.; Ding, X. L.; He, S. G.; Ma, T. M. Structures and Reactivity of Oxygen-Rich Scandium Cluster Anions ScO_{3-5}^-. *ChemPhysChem* **2012**, *13*, 1282−1288.
(17) Zhao, Y. X.; Yuan, J. Y.; Ding, X. L.; He, S. G.; Zheng, W. J. Electronic Structure and Reactivity of a Biradical Cluster: $Sc_3O_6^-$. *Phys. Chem. Chem. Phys.* **2011**, *13*, 10084−10090.
(18) Xu, B.; Zhao, Y. X.; Li, X. N.; Ding, X. L.; He, S. G. Experimental and Theoretical Study of Hydrogen Atom Abstraction from n-Butane by Lanthanum Oxide Cluster Anions. *J. Phys. Chem. A* **2011**, *115*, 10245−10250.
(19) Ma, J. B.; Wu, X. N.; Zhao, Y. X.; Ding, X. L.; He, S. G. Characterization of Mononuclear Oxygen-Centered Radical O^- in $Zr_2O_8^-$ Cluster. *J. Phys. Chem. A* **2010**, *114*, 10024−10027.
(20) Wang, Z.-C.; Yin, S.; Bernstein, E. R. Gas-Phase Neutral Binary Oxide Clusters: Distribution, Structure, and Reactivity toward CO. *J. Phys. Chem. Lett.* **2012**, *3*, 2415−2419.
(21) (a) Ma, J. B.; Wang, Z. C.; Schlangen, M.; He, S. G.; Schwarz, H. Thermal Reactions of $YAlO_3^+$ with Methane: Increasing the Reactivity of $Y_2O_3^+$ and the Selectivity of $Al_2O_3^+$ by Doping. *Angew. Chem., Int. Ed.* **2012**, *51*, 5991−5994. (b) Wang, Z.-C.; Dietl, N.; Kretschmer, R.; Weiske, T.; Schlangen, M.; Schwarz, H. Catalytic Redox Reactions in the CO/N_2O System Mediated by the Bimetallic Oxide-Cluster Couple $AlVO_3^+/AlVO_4^+$. *Angew. Chem., Int. Ed.* **2011**, *50*, 12351−12354. (c) Dietl, N.; Höckendorf, R. F.; Schlangen, M.; Lerch, M.; Beyer, M. K.; Schwarz, H. Generation, Reactivity towards Hydrocarbons, and Electronic Structure of Heteronuclear Vanadium Phosphorous Oxygen Cluster Ions. *Angew. Chem., Int. Ed.* **2011**, *50*, 1430−1434. (d) Zhang, Z.-G.; Xu, H.-G.; Kong, X.-Y.; Zheng, W.-J. Anion Photoelectron Spectroscopy and Density Functional Study of Small Aluminum-Vanadium Oxide Clusters. *J. Phys. Chem. A* **2011**, *115*, 13−18. (e) Zhang, Z.-G.; Xu, H.-G.; Zhao, Y.-C.; Zheng, W.-J. Photoelectron Spectroscopy and Density Functional Theory Study of $TiAlO_y^-$ (y = 1−3) and $TiAl_2O_y^-$ (y = 2−3) Clusters. *J. Chem. Phys.* **2010**, *133*, 154314. (f) Ding, X.-L.; Wu, X.-N.; Zhao, Y.-X.; He, S.-G.; Bond, C-H Activation by Oxygen-Centered Radicals over Atomic Clusters. *Acc. Chem. Res.* **2012**, *45*, 382−390. (g) Wang, Z.-C.; Wu, X.-N.; Zhao, Y.-X.; Ma, J.-B.; Ding, X.-L.; He, S.-G. C-H Activation on Aluminum−Vanadium Bimetallic Oxide Cluster Anions. *Chem.—Eur. J.* **2011**, *17*, 3449−3457. (h) Li, Z.-Y.; Zhao, Y.-X.; Wu, X.-N.; Ding, X.-L.; He, S.-G. Methane Activation by Yttrium-Doped Vanadium Oxide Cluster Cations: Local Charge Effects. *Chem.—Eur. J.* **2011**, *17*, 11728−11733. (i) Zhao, Y.-X.; Wu, X.-N.; Ma, J.-B.; He, S.-G.; Ding, X.-L. Experimental and Theoretical Study of the Reactions between Vanadium-Silicon Heteronuclear Oxide Cluster Anions with n-Butane. *J. Phys. Chem. C* **2010**, *114*, 12271−12279. (j) Wang, Z.-C.; Wu, X.-N.; Zhao, Y.-X.; Ma, J.-B.; Ding, X.-L.; He, S.-G. Room-Temperature Methane Activation by a Bimetallic Oxide Cluster $AlVO_4^+$. *Chem. Phys. Lett.* **2010**, *489*, 25−29. (k) Ma, J. B.; Wu, X. N.; Zhao, Y. X.; Ding, X. L.; He, S. G. Methane Activation by $V_3PO_{10}^+$ and $V_4O_{10}^+$ Clusters: a Comparative Study. *Phys. Chem. Chem. Phys.* **2010**, *12*, 12223−12228.
(22) (a) He, S. G.; Xie, Y.; Guo, Y.; Bernstein, E. R. Formation, Detection, and Stability Studies of Neutral Vanadium Sulfide Clusters. *J. Chem. Phys.* **2007**, *126*, 194315. (b) Matsuda, Y.; Bernstein, E. R. Identification, Structure, and Spectroscopy of Neutral Vanadium Oxide Clusters. *J. Phys. Chem. A* **2005**, *109*, 3803−3811. (c) Matsuda, Y.; Bernstein, E. R. On the Titanium Oxide Neutral Cluster Distribution in the Gas Phase: Detection through 118 nm Single-Photon and 193 nm Multiphoton Ionization. *J. Phys. Chem. A* **2004**, *109*, 314−319.
(23) Xue, W.; Wang, Z.-C.; He, S.-G.; Xie, Y.; Bernstein, E. R. Experimental and Theoretical Study of the Reactions between Small Neutral Iron Oxide Clusters and Carbon Monoxide. *J. Am. Chem. Soc.* **2008**, *130*, 15879−15888.
(24) (a) Dong, F.; Heinbuch, S.; Xie, Y.; Bernstein, E. R.; Rocca, J. J.; Wang, Z. C.; Ding, X. L.; He, S. G. C═C Bond Cleavage on Neutral $VO_3(V_2O_5)_n$ Clusters. *J. Am. Chem. Soc.* **2009**, *131*, 1057−1066. (b) Dong, F.; Heinbuch, S.; Xie, Y.; Rocca, J. J.; Bernstein, E. R.; Wang, Z.-C.; Deng, K.; He, S.-G. Experimental and Theoretical Study of the Reactions Between Neutral Vanadium Oxide Clusters and Ethane, Ethylene, and Acetylene. *J. Am. Chem. Soc.* **2008**, *130*, 1932−1943.
(25) Wang, Z.-C.; Xue, W.; Ma, Y.-P.; Ding, X.-L.; He, S.-G.; Dong, F.; Heinbuch, S.; Rocca, J. J.; Bernstein, E. R. Partial Oxidation of Propylene Catalyzed by VO_3 Clusters: A Density Functional Theory Study. *J. Phys. Chem. A* **2008**, *112*, 5984−5993.
(26) He, S.-G.; Xie, Y.; Dong, F.; Heinbuch, S.; Jakubikova, E.; Rocca, J. J.; Bernstein, E. R. Reactions of Sulfur Dioxide with Neutral Vanadium Oxide Clusters in the Gas Phase. II. Experimental Study Employing Single-Photon Ionization. *J. Phys. Chem. A* **2008**, *112*, 11067−11077.
(27) Heinbuch, S.; Dong, F.; Rocca, J. J.; Bernstein, E. R. Experimental and Theoretical Studies of Reactions of Neutral Vanadium and Tantalum Oxide Clusters with NO and NH_3. *J. Chem. Phys.* **2010**, *133*, 174314.
(28) Dong, F.; Heinbuch, S.; Xie, Y.; Rocca, J. J.; Bernstein, E. R. Reactions of Neutral Vanadium Oxide Clusters with Methanol. *J. Phys. Chem. A* **2009**, *113*, 3029−3040.
(29) (a) Xie, Y.; Dong, F.; Heinbuch, S.; Rocca, J. J.; Bernstein, E. R. Oxidation Reactions on Neutral Cobalt Oxide Clusters: Experimental and Theoretical Studies. *Phys. Chem. Chem. Phys.* **2010**, *12*, 947−959. (b) He, S. G.; Xie, Y.; Dong, F.; Bernstein, E. R. Reaction of Niobium and Tantalum Neutral Clusters with Low Pressure, Unsaturated Hydrocarbons in a Pickup Cell: From Dehydrogenation to Met-Car Formation. *J. Chem. Phys.* **2006**, 125. (c) Shin, D. N.; Matsuda, Y.; Bernstein, E. R. On the Iron Oxide Neutral Cluster Distribution in the Gas Phase. II - Detection Through 118 nm Single Photon Ionization. *J. Chem. Phys.* **2004**, *120*, 4157−4164. (d) Yin, S.; Xie, Y.; Bernstein, E. R. Experimental and Theoretical Studies of Ammonia Generation: Reactions of H_2 with Neutral Cobalt Nitride Clusters. *J. Chem. Phys.* **2012**, *137*, 124304−124308.
(30) Frisch, M. J.; Trucks, G. W.; Schlegel, H. B.; Scuseria, G. E.; Robb, M. A.; Cheeseman, J. R.; Scalmani, G.; Barone, V.; Mennucci, B.; Petersson, G. A.; et al. *Gaussian 09*, Revision C.01; Gaussian, Inc.: Wallingford, CT, 2009.
(31) (a) Becke, A. D. Density-Functional Exchange-Energy Approximation with Correct Asymptotic-Behavior. *Phys. Rev. A* **1988**, *38*, 3098−3100. (b) Lee, C. T.; Yang, W. T.; Parr, R. G. Development of the Colle-Salvetti Correlation-Energy Formula into a Functional of the Electron-Density. *Phys. Rev. B: Condens. Matter Mater. Phys.* **1988**, *37*, 785−789. (c) Becke, A. D. Density-Functional

Thermochemistry. 3. The Role of Exact Exchange. *J. Chem. Phys.* **1993**, *98*, 5648−5652.
(32) Kohn, W.; Sham, L. J. Self-Consistent Equations Including Exchange and Correlation Effects. *Phys. Rev.* **1965**, *140*, A1133.
(33) Schafer, A.; Huber, C.; Ahlrichs, R. Fully Optimized Contracted Gaussian-Basis Sets of Triple Zeta Valence Quality for Atoms Li to Kr. *J. Chem. Phys.* **1994**, *100*, 5829−5835.
(34) Wang, Z. C.; Ding, X. L.; Ma, Y. P.; Cao, H.; Wu, X. N.; Zhao, Y. X.; He, S. G. Theoretical Study of Partial Oxidation of Ethylene by Vanadium Trioxide Cluster Cation. *Chin. Sci. Bull.* **2009**, *54*, 2814−2821.
(35) Pykavy, M.; van Wullen, C.; Sauer, J. Electronic Ground States of the $V_2O_4^{+/0/-}$ Species from Multireference Correlation and Density Functional Studies. *J. Chem. Phys.* **2004**, *120*, 4207−4215.
(36) (a) Zhao, Y. X.; Ding, X. L.; Ma, Y. P.; Wang, Z. C.; He, S. G. Transition Metal Oxide Clusters with Character of Oxygen-Centered Radical: a DFT Study. *Theo. Chem. Acc.* **2010**, *127*, 449−465. (b) Ma, J. B.; Zhao, Y. X.; He, S. G.; Ding, X. L. Experimental and Theoretical Study of the Reactions between Vanadium Oxide Cluster Cations and Water. *J. Phys. Chem. A* **2012**, *116*, 2049−2054. (c) Jia, M. Y.; Xu, B.; Ding, X. L.; Zhao, Y. X.; He, S. G.; Ge, M. F. Experimental and Theoretical Study of the Reactions between Vanadium Oxide Cluster Cations and Hydrogen Sulfide. *J. Phys. Chem. C* **2012**, *116*, 9043−9048.
(37) (a) Rozanska, X.; Sauer, J. Oxidative Dehydrogenation of Hydrocarbons by $V_3O_7^+$ Compared to Other Vanadium Oxide Species. *J. Phys. Chem. A* **2009**, *113*, 11586−11594. (b) Sauer, J.; Dobler, J. Structure and Reactivity of V_2O_5: Bulk Solid, Nanosized Clusters, Species Supported on Silica and Alumina, Cluster Cations and Anions. *Dalton Trans.* **2004**, 3116−3121.
(38) Ma, Y. P.; Ding, X. L.; Zhao, Y. X.; He, S. G.; Theoretical, A. Study on the Mechanism of C_2H_4 Oxidation over a Neutral V_3O_8 Cluster. *ChemPhysChem* **2010**, *11*, 1718−1725.
(39) (a) Santambrogio, G.; Brummer, M.; Woste, L.; Döbler, J.; Sierka, M.; Sauer, J.; Meijer, G.; Asmis, K. R. Gas Phase Vibrational Spectroscopy of Mass-Selected Vanadium Oxide Anions. *Phys. Chem. Chem. Phys.* **2008**, *10*, 3992−4005. (b) Asmis, K. R.; Santambrogio, G.; Brummer, M.; Sauer, J. Polyhedral Vanadium Oxide Cages: Infrared Spectra of Cluster Anions and Size-Induced d Electron Localization. *Angew. Chem., Int. Ed.* **2005**, *44*, 3122−3125. (c) Zhai, H. J.; Dobler, J.; Sauer, J.; Wang, L. S. Probing the Electronic Structure of Early Transition-Metal Oxide Clusters: Polyhedral Cages of $(V_2O_5)_n^-$ (n = 2−4) and $(M_2O_5)_2^-$ (M = Nb, Ta). *J. Am. Chem. Soc.* **2007**, *129*, 13270−13276.
(40) (a) Schroder, D.; Engeser, M.; Schwarz, H.; Rosenthal, E. C. E.; Dobler, J.; Sauer, J. Degradation of Ionized $OV(OCH3)_3$ in the Gas Phase. From the Neutral Compound all the Way Down to the Quasi-Terminal Fragments VO^+ and VOH^+. *Inorg. Chem.* **2006**, *45*, 6235−6245. (b) Schroder, D.; Loos, J.; Engeser, M.; Schwarz, H.; Jankowiak, H. C.; Berger, R.; Thissen, R.; Dutuit, O.; Dobler, J.; Sauer, J. Ion Chemistry of $OV(OCH3)_3$ in the Gas Phase: Molecular Cations and Anions and Their Primary Fragmentations. *Inorg. Chem.* **2004**, *43*, 1976−1985.
(41) Schlegel, H. B. Optimization of Equilibrium Geometries and Transition Structures. *J. Comput. Chem.* **1982**, *3*, 214−218.
(42) Peng, C.; Ayala, P. Y.; Schlegel, H. B.; Frisch, M. J. Using Redundant Internal Coordinates to Optimize Equilibrium Geometries and Transition States. *J. Comput. Chem.* **1996**, *17*, 49−56.
(43) (a) Gonzalez, C.; Schlegel, H. B. Reaction Path Following in Mass-Weighted Internal Coordinates. *J. Phys. Chem.* **1990**, *94*, 5523−5527. (b) Gonzalez, C.; Schlegel, H. B. An Improved Algorithm for Reaction-Path Following. *J. Chem. Phys.* **1989**, *90*, 2154−2161. (c) Truhlar, D. G.; Gordon, M. S. From Force Fields to Dynamics: Classical and Quantal Paths. *Science* **1990**, *249*, 491−498.
(44) Schlangen, M.; Schwarz, H. Effects of Ligands, Cluster Size, and Charge State in Gas-Phase Catalysis: A Happy Marriage of Experimental and Computational Studies. *Catal. Lett.* **2012**, *142*, 1265−1278.
(45) Zhao, Y. X.; Wu, X. N.; Ma, J. B.; He, S. G.; Ding, X. L. Characterization and Reactivity of Oxygen-Centred Radicals over Transition Metal Oxide Clusters. *Phys. Chem. Chem. Phys.* **2011**, *13*, 1925−1938.